

# Numerical study of simultaneous heat and mass transfer in absorption of vapor in laminar liquid film

Sara Armou<sup>\*1</sup>, Rachid Mir<sup>2</sup>, Youness El hammami<sup>3</sup>, Sakina El hamdani<sup>4</sup>,  
Kaoutar Zine-Dine<sup>5</sup>

<sup>1,2,3,4,5</sup> Laboratory of Mechanics, Processes, Energy and Environment, National School of Applied Sciences  
ENSA, B.P 1136, AGADIR, MOROCCO

---

## ABSTRACT

A numerical investigation has been performed to study the combined heat and mass transfer in a falling liquid film absorption in aqueous lithium bromide solution flowing downward inside a vertical channel. The parabolic governing equations are solved for steady, two-dimensional laminar flow using the finite volume method. In the studied model, the coolant flows from bottom to top of the plate on which trickles film rich solution of lithium bromide and water vapor is absorbed by the film at the interface liquid-vapor. The heat release at the interface being mainly due to the water vapor phase change enthalpy. The numerical results indicate that the temperature distribution is the lowest at the wall and increases to the highest at the interface due to the heat absorption released at the interface and the concentration distribution is the highest at the wall and decreases to the lowest at the interface due to the water vapor absorbed at the interface. The effects of operating condition are presented and discussed and the result show that the absorption mass flux is higher for lower Reynolds number and increases with the increase of the inlet solution concentration, the system pressure and with the decrease of the inlet cooling water temperature.

**Keywords:** Absorption process, Falling film, Heat and mass transfer, Lithium bromide, Numerical simulation.

---

## 1. INTRODUCTION

The cold is used in various forms in large number industrial sectors and currently occurs with a compression system that uses electricity as important source of energy. These systems use refrigerants that have destructive effects, for these reasons it was necessary to use the absorption machines that represent an economical and efficient alternative for compression machines. Absorption refrigeration systems use fluids environmentally citing lithium bromide, ammonia, water or alcohols. The absorption machines are now the most widespread thermal refrigeration systems in several applications in the industry. These machines are running with an absorber, which is the most important element of the system which has a direct effect on efficiency, size, and manufacturing and operating costs of the system.

The development of absorption heat pump requires a better understanding of the combined heat and mass transfer process in absorption of LiBr/H<sub>2</sub>O. Many works concerning the study of falling film absorption have been made and from these works one can mention those of:

Shahram Karami et al. [1] numerically studied using the finite difference method the heat transfer and mass process in the steam absorption in a solution of LiBr, water-cooled on an inclined plate of the absorber. They found that the mass rate of absorption and the heat transfer and mass coefficients increase as the angle of the plate increases. Icksoo Kyung et al. [2] developed a model for the absorption of water vapor by the LiBr aqueous solution on a smooth horizontal tube using three different flow regimes. The calculation indicates the importance of droplet formation regime for predicting the absorber performance. K. J. Kim et al. [3] experiments were conducted on the water vapor absorption in an aqueous solution of lithium bromide (50% to 60% by mass) in the form of film flow on a vertical surface, while their results showed that the mass transfer coefficients are not different between 50% and 60% by weight LiBr solution. Shoushi Bo et al. [4] numerically investigated absorption process in the liquid film using CFD software package-Fluent, they have posed the convective boundary condition on the cooling water side and they have also studied the effect of variable physical properties on the process. The result is the overall rate of mass transfer of absorption is approximately 6.5% higher when properties are assumed constant. Raisul Islam et al. [5] experimentally studied two absorbers in similar conditions. The maximum increase of the steam vapor mass flow for the film-inverting design was about 100% compared to that of the tubular absorber. Marc Medrano et al. [6] have carried out an experimental study of the falling

film absorption of aqueous solution of lithium bromide inside a vertical tube. They have found that in water-cooling thermal conditions the mass absorption fluxes are in the interval  $0.001\text{--}0.0015 \text{ kg}\cdot\text{m}^{-2}\cdot\text{s}^{-1}$  while in air-cooling thermal conditions the interval of mass absorption values decreases to  $0.00030\text{--}0.00075 \text{ kg}\cdot\text{m}^{-2}\cdot\text{s}^{-1}$ . Liu Yang et al. [7] developed numerical model for the absorption of ammonia on a falling film for different ammonia-water mixtures containing nanoparticles and dispersants. The results show that when absorption pressure decreases or when initial concentration of mixture increases, the relative intensity of effect on absorption rate is weakened by the variation of thermal conductivity but enhanced by the variation of mass transfer coefficients and flow resistance, while the variation of mixture's viscosity exhibits very low effect.

The present work focused on the simulation of the heat and mass transfer during absorption of vapor into liquid film of LiBr falling along a vertical channel. The conservation equations were used to determine velocity, temperature and concentration distribution within the film-thickness using the finite volume method. Effects of the four independent variables such as film Reynolds number, inlet solution concentration, inlet pressure and inlet cooling water temperature on absorption mass flux are presented in this paper.

## 2. MODEL DESCRIPTION

### A. Physical model for absorber

The model of the problem studied is illustrated in Fig.1. At the top of the channel, a liquid solution is introduced; it flows down over vertical plate as a thin film of aqueous solution of lithium bromide, composed of absorbent (LiBr) and refrigerant ( $\text{H}_2\text{O}$ ). The mass transfer process occurs at the interface of liquid film and vapor from the evaporator. The vapor is absorbed by the film and the heat produced due to this exothermic transformation is rejected by the external cooling water which flows countercurrent to the falling liquid film inside the channel.

The following assumptions have been taken into account in the formulation of the problem:

- The equilibrium condition exists at the interface.
- No shear forces are exerted on the liquid by the vapor.
- The flow of liquid film is considered laminar.
- The film thickness is considered constant.
- Heat transfer in the vapor phase is negligible compared to that in the liquid phase.
- The radiative transfer is negligible.
- Heat and mass transfer are two-dimensional.

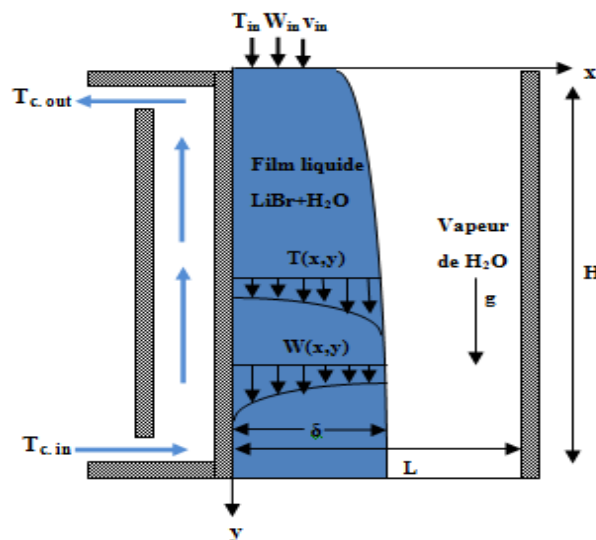


Figure 1. Physical model

### B. Mathematical modeling

Taking account of assumptions mentioned above, the governing equations described the flow and the heat and mass transfers corresponding to the continuity, momentum, energy and concentration in the liquid phase can be written as:  
Continuity equation:

$$\frac{\partial}{\partial x}(\rho u) + \frac{\partial}{\partial y}(\rho v) = 0 \quad (1)$$

X-momentum equation:

$$\frac{\partial(\rho uu)}{\partial x} + \frac{\partial(\rho v u)}{\partial y} = \frac{\partial}{\partial x} \left( \mu \frac{\partial u}{\partial x} \right) + \frac{\partial}{\partial y} \left( \mu \frac{\partial u}{\partial y} \right) \quad (2)$$

Y-momentum equation:

$$\frac{\partial(\rho u v)}{\partial x} + \frac{\partial(\rho v v)}{\partial y} = \frac{\partial}{\partial x} \left( \mu \frac{\partial v}{\partial x} \right) + \frac{\partial}{\partial y} \left( \mu \frac{\partial v}{\partial y} \right) + \rho g \quad (3)$$

Energy equation:

$$\frac{\partial(\rho c_p u T)}{\partial x} + \frac{\partial(\rho c_p v T)}{\partial y} = \frac{\partial}{\partial x} \left( \lambda \frac{\partial T}{\partial x} \right) + \frac{\partial}{\partial y} \left( \lambda \frac{\partial T}{\partial y} \right) + \frac{\partial}{\partial x} \left( \rho D (c_{p1} - c_{p2}) \frac{\partial W}{\partial x} T \right) \quad (4)$$

Concentration equation:

$$\frac{\partial(\rho u W)}{\partial x} + \frac{\partial(\rho v W)}{\partial y} = \frac{\partial}{\partial x} \left( \rho D \frac{\partial W}{\partial x} \right) + \frac{\partial}{\partial y} \left( \rho D \frac{\partial W}{\partial y} \right) \quad (5)$$

Where  $\rho$ ,  $u$ ,  $v$ ,  $T$ ,  $W$ ,  $\mu$ ,  $c_p$ ,  $\lambda$  and  $D$  are respectively, density, axial velocity, transverse velocity, temperature, mass fraction LiBr in solution, dynamic viscosity, specific heat capacity, thermal conductivity and mass diffusivity;  $c_{p1}$  and  $c_{p2}$  are the specific heat capacity of lithium bromide and water respectively and  $g$  is the gravitational acceleration.

The film thickness is determined by Nusselt [8] theory and it's described by the equation:

$$\delta = \left( \frac{3\Gamma\mu}{\rho^2 g} \right)^{\frac{1}{3}} \quad (6)$$

#### • Boundary conditions

The liquid phase equations (1)-(5) are subjected to the following boundary conditions:

**Conditions to entry:**  $y = 0$  and  $0 \leq x \leq \delta$

At the inlet of the liquid film, the temperature and concentration of the film are uniform.

$$T = T_{in}, W = W_{in}, v = v_{in} \text{ and } u = 0 \quad (7)$$

**Conditions at the wall:**  $0 \leq y \leq H$  and  $x = 0$

At the surface of wall, we have the no-slip and impermeable condition, so the gradient of concentration and the flow velocity are equal to zero.

$$T = T_w, \frac{\partial W}{\partial x} = 0, v = 0 \text{ and } u = 0 \quad (8)$$

The wall temperature changes linearly and it's determined by the equation as follows

$$T_w = T_{c,in} + \left( \frac{H-y}{H} \right) \times (T_{c,out} - T_{c,in})$$

**Conditions at the interface:**  $0 \leq y \leq H$  and  $x = \delta$

Interface equilibrium concentration can be obtained by a function of interface temperature and vapor pressure [9]:

$$\text{Log}_{10} P = A + \frac{B}{T} + \frac{C}{T^2} \quad (9)$$

Where

$$A = a_0 + a_1 W + a_2 W^2 + a_3 W^3$$

$$B = b_0 + b_1 W + b_2 W^2 + b_3 W^3$$

$$C = c_0 + c_1 W + c_2 W^2 + c_3 W^3$$

Equation (9) was solved iteratively using the Newton-Raphson root search method.

The continuity of energy at the vapor–liquid interface is expressed as follows:

$$\lambda \left. \frac{\partial T}{\partial x} \right|_{x=\delta} = \dot{m} \times H_{abs} \quad (10)$$

$H_{abs}$  is the heat of absorption.

Where the interfacial absorption mass flux is calculated by the following equation:

$$\dot{m} = \frac{-\rho D}{W_{surf}} \left( \frac{\partial W}{\partial x} \right)_{x=\delta} \quad (11)$$

Continuity of shear stress:

$$\mu \left. \frac{\partial v}{\partial x} \right|_{x=\delta} = 0 \quad (12)$$

The velocity in x-direction:

$$u = \frac{D}{W_{surf}} \left( \frac{\partial W}{\partial x} \right)_{x=\delta} \quad (13)$$

**Conditions at the outlet:**  $y = H$  and  $0 \leq x \leq \delta$

$$\frac{\partial T}{\partial y} = 0, \quad \frac{\partial W}{\partial y} = 0, \quad \frac{\partial u}{\partial y} = 0 \quad \text{and} \quad \frac{\partial v}{\partial y} = 0 \quad (14)$$

The local heat transfer coefficient from the interface to bulk solution along the film flow is expressed in terms of Nusselt number:

$$Nu_{ib} = \frac{h_{ib} \delta}{\lambda} = \frac{\delta}{(T_{surf} - T_b)} \left. \frac{\partial T}{\partial x} \right|_{x=\delta}$$

The local heat transfer coefficient from the bulk solution to tube wall surface along the film flow is expressed in terms of Nusselt number:

$$Nu_{bw} = \frac{h_{bw} \delta}{\lambda} = \frac{\delta}{(T_b - T_w)} \left. \frac{\partial T}{\partial x} \right|_{x=0}$$

The local mass transfer coefficient from the interface to bulk solution along the film flow is expressed in terms of Sherwood number:

$$Sh = \frac{h_m \delta}{D} = \frac{\delta}{W_{surf} (W_{surf} - W_b)} \left. \frac{\partial W}{\partial x} \right|_{x=\delta}$$

The bulk temperature and bulk mass fraction are defined as follows:

$$T_b = \frac{\int_0^\delta \rho c_p u T dx}{\int_0^\delta \rho c_p u dx} \quad ; \quad W_b = \frac{\int_0^\delta \rho c_p u W dx}{\int_0^\delta \rho c_p u dx}$$

### 3. NUMERICAL METHOD AND GRID SIZE EFFECT

The system of equations (1)-(5) describing the heat and mass transfer with boundary conditions were discretized by finite volume method proposed by Patankar [10]. Integrating the governing equations, we obtained a system of algebraic equations written in the following compact form:

$$a_P \Phi_P = a_E \Phi_E + a_W \Phi_W + a_N \Phi_N + a_S \Phi_S + b$$

With:  $\Phi = (u, v, T, W)$

We introduced an interpolation scheme for determining the values of the coefficients of the linear system; the coefficients  $a_P, a_E, a_W, a_N, a_S$  are obtained by using a power law interpolation scheme. The sweeping method line by line, with the algorithm of Thomas was used for the iterative resolution of the systems of equations. The convergence criterion is that the maximal residual is less than  $10^{-7}$ . A uniform grid was used in the domain with IN nodes in the

transversal direction and JN nodes in the axial direction. To choose the best mesh that allows having the most accurate results, we studied respectively the influence of the grid size on the interface to bulk liquid heat transfer coefficient presented in Fig. 2 (a) and on the local Nusselt number shown in Fig. 2 (b). So we adopted for reasons of calculation accuracy a  $201 \times 61$  mesh.

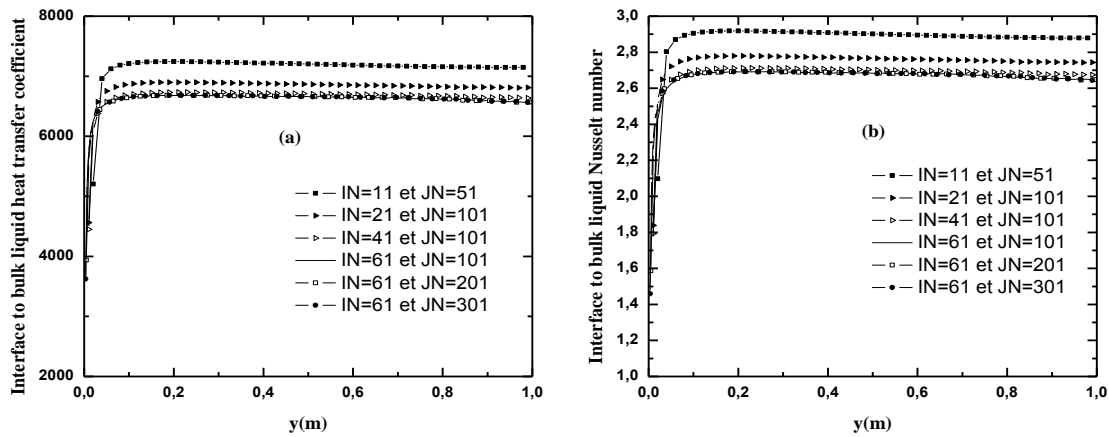


Figure 2. Influence of the grid size on. (a) the Interface to bulk liquid heat transfer coefficient and (b) the local Nusselt number

#### 4. NUMERICAL RESULTS AND DISCUSSION

The main parameters of operating conditions used in the calculation in the present study are listed in Tab.1 and the physical properties of LiBr solution used are collected from[9]:

Table 1: Operating conditions

Parameters	Ranges
Inlet solution temperature $T_{in}$	45°C
Inlet solution concentration $W_{in}$	0.58-0.62
Reynolds number $Re_{in}$	10-100
Inlet pressure $P_{in}$	0.5KPa-1KPa
Plate height H	1m
Inlet cooling water temperature $T_{c,in}$	32°C
Outlet cooling water temperature $T_{c,out}$	36°C

#### C. Validation of numerical model

In order to verify the accuracy of the numerical procedure, a computer code were validated by comparing the results obtained on numerical study from the present model and those reported by Kawae et al. [11] and Yoon et al. [12]. A very satisfied agreement was observed between the different results. The small differences observed between the two results in terms of values of mass flux, temperature and concentration at the interface is less than 1%.

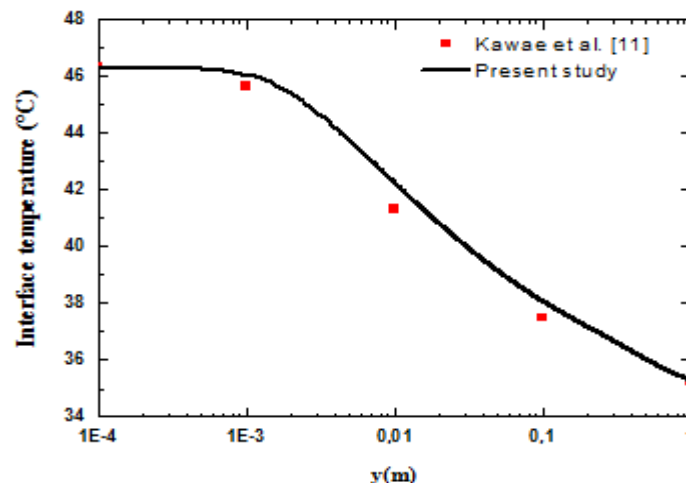


Figure 3. Comparison of interfacial temperature of present study with Kawae et al. [11]

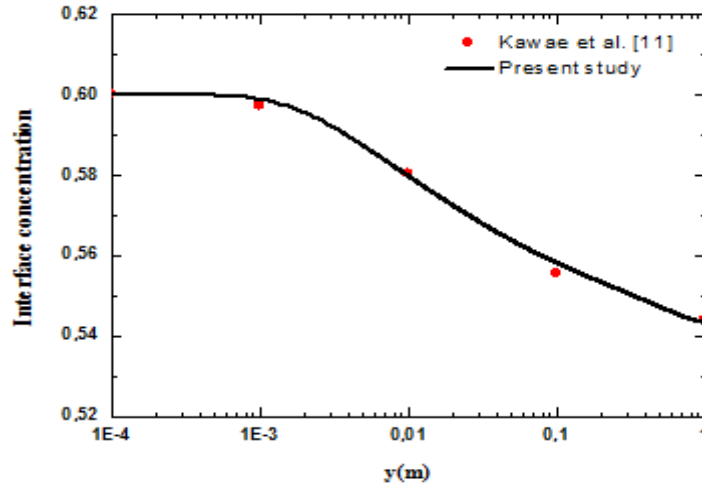


Figure 4. Comparison of interfacial concentration of present study with Kawae et al. [11]

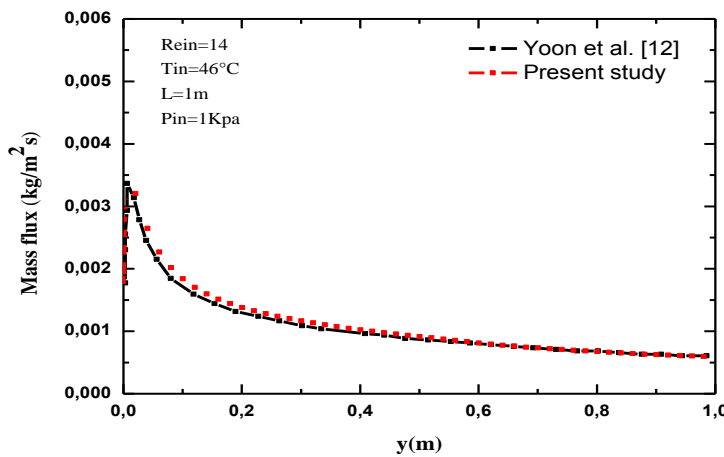


Figure 5. Comparison of mass flux of present study with Yoon et al. [12]

#### D. Temperature and concentration profiles

The profiles temperature Fig. 6 (a) is the lowest at the wall and increases to the highest at the interface liquid-vapor due the heat absorption liberated at the interface. The temperature gradient is high at the inlet and decreases toward the exit of the channel. The concentration profiles for different location are shown in Fig. 6 (b), from the wall it can be seen that the concentration at the inlet remains constant; by approaching to the interface the vapor absorbed by liquid film reduces the concentration. The concentration gradient is high at the inlet and decreases toward the exit of the channel, due to end of the absorption.

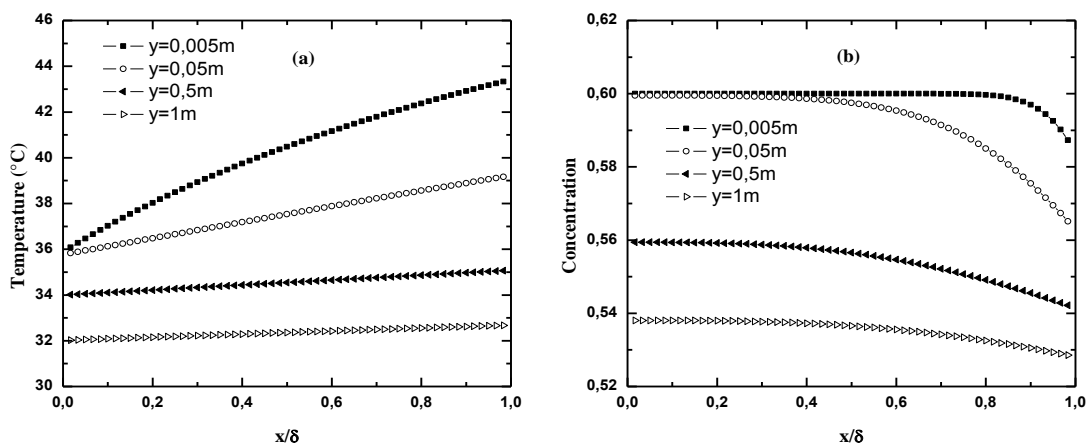


Figure 6. Temperature profile (a) and concentration profile (b) across liquid film at  $T_{in}=45^{\circ}C$ ,  $W_{in}=0.6$ ,  $Re_{in}=10$  and  $P_{in}=1KPa$

Fig. 7 (a) and (b) present the variation of temperature and concentration along the liquid film. The interface temperature is varying rapidly near the inlet region but gradually as the long of the plate increase due the heat absorption released at the interface, while the wall temperature varied linearly and the bulk temperature decreases slowly as y increases. Similar distributions are spotted for the interface, bulk and wall concentration, the interface concentration decrease due the absorbed mass of vapor, the bulk concentration decreases at a slower rate because the mass boundary layer propagates slowly into the film due to low mass diffusivity. From  $y=0.2$  all concentrations decrease linearly along the plate.

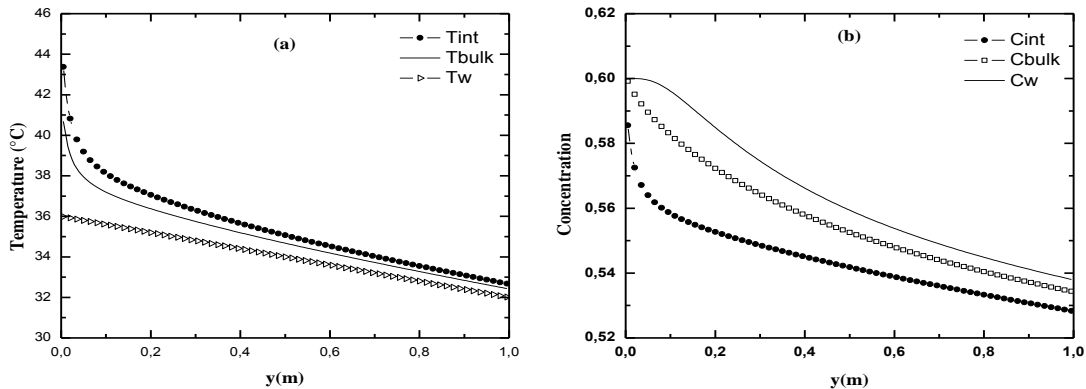


Figure 7. Temperature profile (a) and concentration profile (b) along the plate at  $T_{in}=45^{\circ}\text{C}$ ,  $W_{in}=0.6$ ,  $Re_{in}=10$  and  $P_{in}=1\text{KPa}$

### E. Effect of operating condition

We present a study of the effect of various operating parameters on the absorption process of water vapor into the falling film liquid of lithium bromide in a vertical canal, by varying successively the parameters listed in Tab. 1.

#### 1. Effect of Reynolds Number on heat and mass transfer

The graphs in Fig. 8 and Fig. 9, present the effects of changing Reynolds number on the variation of the solution temperature and concentration respectively along the falling film at interface. According to these figures, for the lower Reynolds number the temperature and the concentration interface decreases rapidly and reaches respectively values  $38^{\circ}\text{C}$  and  $0.56$  until  $y=0.1$  and after the temperature and concentration interface gradient begin to be smaller. At the inlet of the liquid film, the LiBr solution was chosen in a thermodynamic equilibrium state, the vapor pressure driving force is zero. After coming into the inlet, the liquid film starts to become cooled (Fig. 8) by cooling water, which lowers saturation pressure and hence the vapor pressure driving force increases and therefore the interface concentration and the absorption mass flux (Fig. 9 and Fig. 10) consequently begin to respectively increase and decrease. However, once the vapor has been absorbed, the driving force is liquid-side-controlled because of the high resistance to mass diffusion so the vapor pressure driving force to decrease whereas the cooling water causes the vapor pressure driving force to increase. Consequently, the vapor pressure driving force slowly increases and reaches to its maximum value and hence, at this location, the absorption mass flux reaches its maximum value (Fig. 10). By increasing Reynolds number, the solution film thickness increases so the heat transfer between the liquid film and cooling water decreases and hence the mass flux decreases with the increase of Re number only in the region near the inlet. However, in the region of y greater than nearly  $0.2\text{m}$ , the mass flux increases with the increase of Reynolds number as shown in Fig. 10.

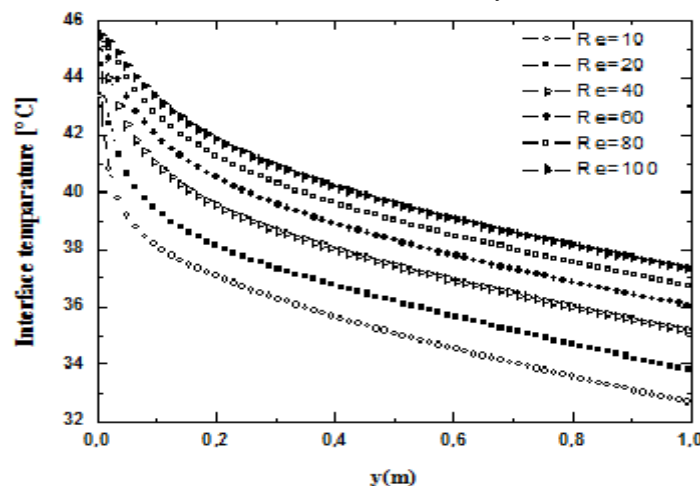


Figure 8. Variation of interface temperature along falling film for different Reynolds number at  $T_{in}=45^{\circ}\text{C}$ ,  $W_{in}=0.6$  and  $P_{in}=1\text{KPa}$



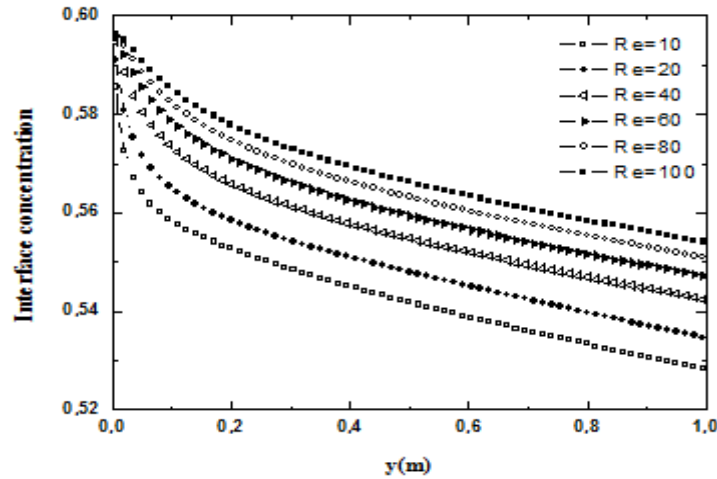


Figure 9. Variation of interface concentration along falling film for different Reynolds number at  $T_{in}=45^{\circ}\text{C}$ ,  $W_{in}=0.6$  and  $P_{in}=1\text{KPa}$

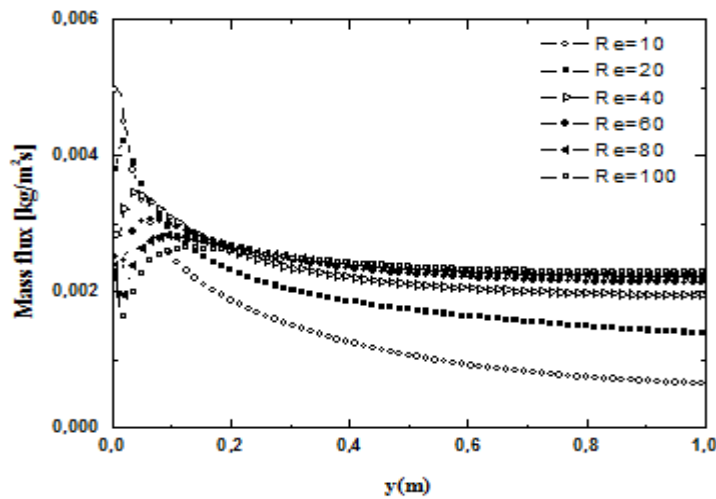


Figure 10. Variation of mass flux at interface for different Reynolds number at  $T_{in}=45^{\circ}\text{C}$ ,  $W_{in}=0.6$  and  $P_{in}=1\text{KPa}$

## 2. The effect of inlet concentration on heat and mass transfer

The variation of absorption mass flux for three value of inlet concentration solution ( $W_{in}=0.58$ ;  $W_{in}=0.6$ ;  $W_{in}=0.62$ ) is presented in Fig. 11. The mass flux in the inlet increases with increase in the concentration of the inlet solution, we can explain that an increase in the inlet solution concentration reduces the pressure of water vapor in the solution and the pressure of the driving force of the vapor increases, which causes an increase in absorption rate. Fig. 12 and Fig. 13 show the variation of interface concentration and temperature for different values of inlet solution concentration. The increase of inlet concentration causes more absorption of water vapor into the solution LiBr so to decrease of interface concentration and interface temperature, which may be explained by the results presented in Fig. 11.

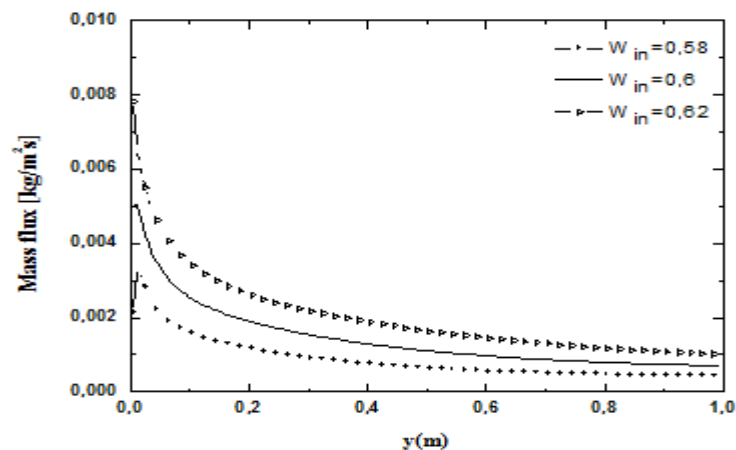


Figure 11. Effect of inlet solution concentration on absorption mass flux at  $T_{in}=45^{\circ}\text{C}$ ,  $Re_{in}=10$  and  $P_{in}=1\text{KPa}$



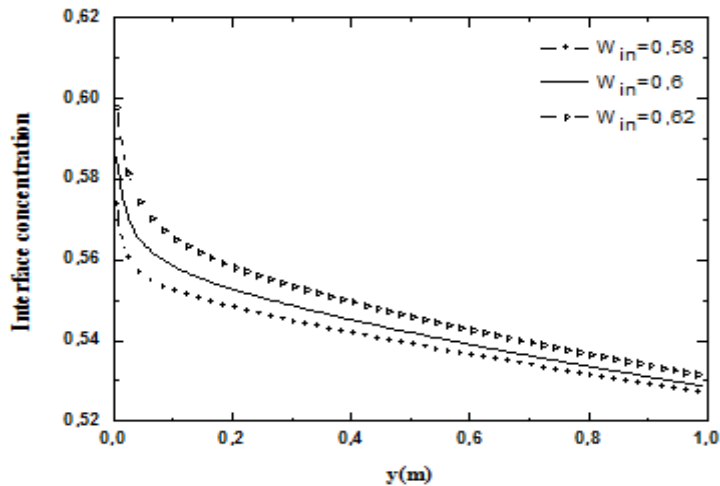


Figure 12. Effect of inlet solution concentration on interface concentration at  $T_{in}=45^{\circ}\text{C}$ ,  $Re_{in}=10$  and  $P_{in}=1\text{KPa}$

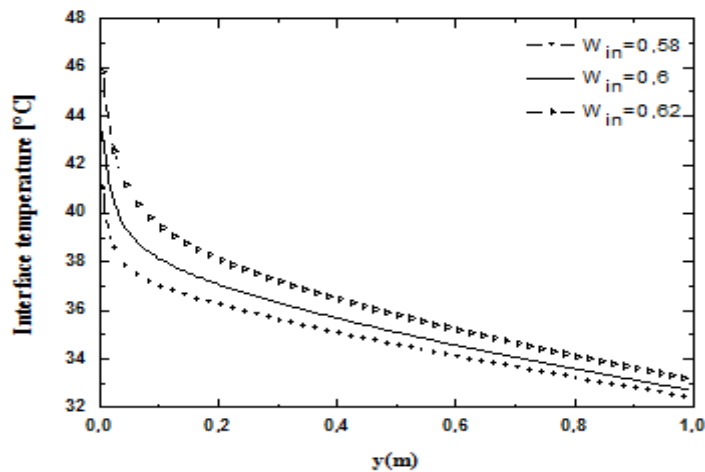


Figure 13. Effect of inlet solution concentration on interface temperature at  $T_{in}=45^{\circ}\text{C}$ ,  $Re_{in}=10$  and  $P_{in}=1\text{KPa}$

### 3. The effect of system pressure on heat and mass transfer

We consider now the following parameters fixed  $W_{in}=0.62$ ;  $T_{in}=45^{\circ}\text{C}$ ;  $Re_{in}=10$  and we studied the influence of the inlet pressure by making change in the range  $P_{in}=0.5\text{-}1\text{KPa}$  the results of the effect of system pressure obtained are illustrated in Fig. 14, Fig. 15 and Fig. 16. It shows that an increase in  $P_{in}$  increases the mass flux as shown in Fig. 14, That can be explain when the inlet pressure increases, the driving force of pressure vapor increases so that the vapor is rapidly absorbed by LiBr solution which leads to decrease of interface concentration (Fig. 15) and a decrease of interface temperature (Fig. 16). So the driving force of pressure vapor is considered a qualitative measure of the mass transfer. Thus, a higher absorber pressure is desirable for the improvement of the heat and mass transfer process.

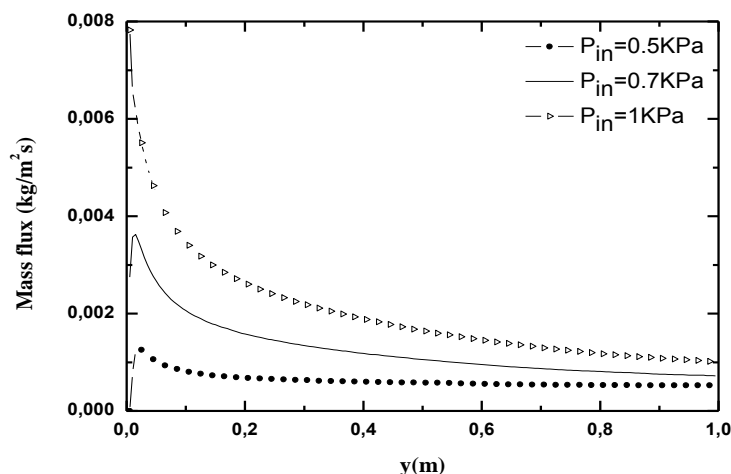


Figure 14. Effect of inlet pressure on absorption mass flux at  $T_{in}=45^{\circ}\text{C}$ ,  $W_{in}=0.62$  and  $Re_{in}=10$

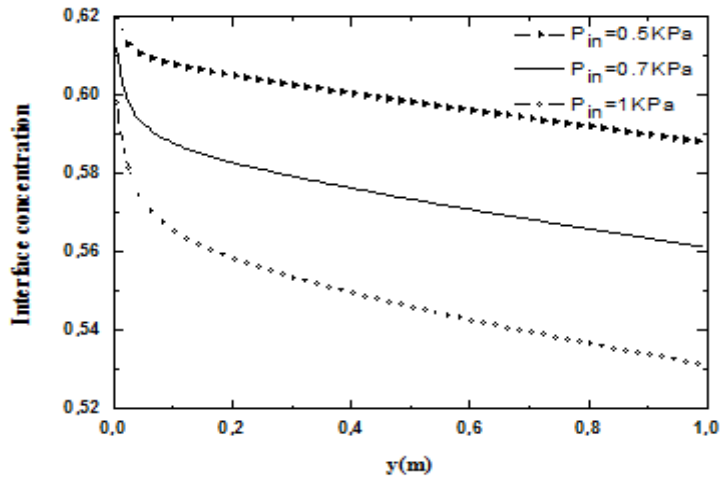


Figure 15. Effect of inlet pressure on interface concentration at  $T_{in}=45^{\circ}\text{C}$ ,  $W_{in}=0.62$  and  $Re_{in}=10$

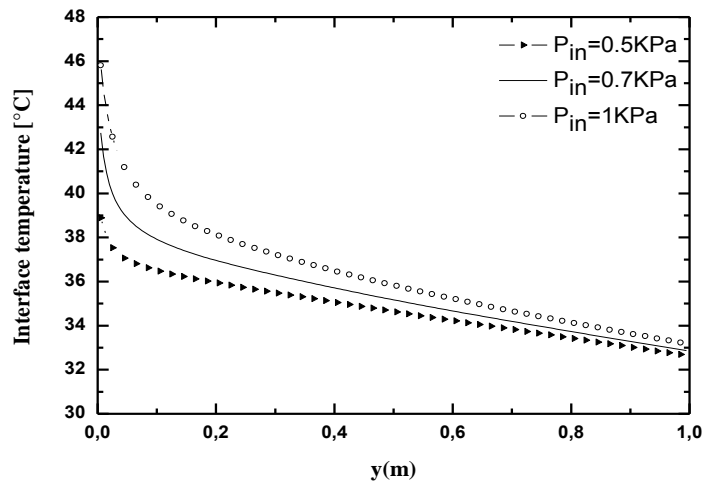


Figure 16. Effect of inlet pressure on interface temperature at  $T_{in}=45^{\circ}\text{C}$ ,  $W_{in}=0.62$  and  $Re_{in}=10$

#### 4. The effect of inlet cooling water temperature on heat and mass transfer

By adopting the following parameters constant:  $P_{in}=1\text{KPa}$ ;  $Re_{in}=10$ ,  $W_{in}=0.62$  and  $T_{in}=45^{\circ}\text{C}$ , we study the effect of the inlet cooling water temperature.

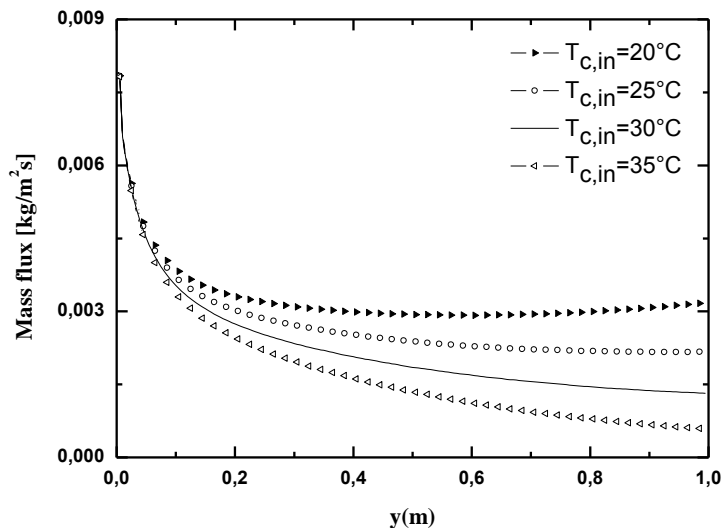


Figure 17. Effect of inlet cooling water temperature on local mass flux at  $T_{in}=45^{\circ}\text{C}$ ,  $W_{in}=0.62$ ,  $Re_{in}=10$  and  $P_{in}=1\text{KPa}$

The variation of absorbed mass flux, interface concentration and interface temperature for different values of inlet cooling water temperature are shown in Fig. 17, Fig. 18 and Fig. 19, it is noticed from Fig. 17, that the absorbed mass flux is more important for  $T_{c,in}=20^{\circ}\text{C}$ . This explains that the absorption is favorable when  $T_{c,in}$  is smaller, this is confirmed by Fig. 18 and Fig. 19 which show the decrease of interface concentration and interface temperature in the inlet of the plate by decreasing  $T_{c,in}$ . It can be said that the increase in the inlet cooling water temperature improves the absorption rate of the water vapor.

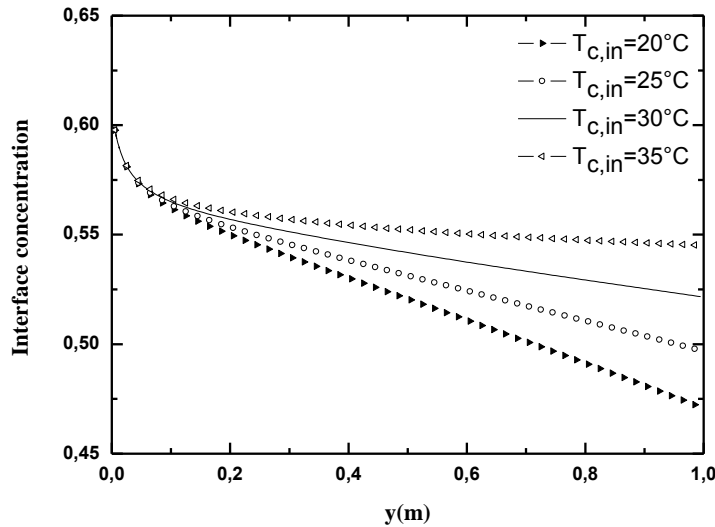


Figure 18. Effect of inlet cooling water temperature on interface concentration at  $T_{in}=45^{\circ}\text{C}$ ,  $W_{in}=0.62$ ,  $Re_{in}=10$  and  $P_{in}=1\text{KPa}$

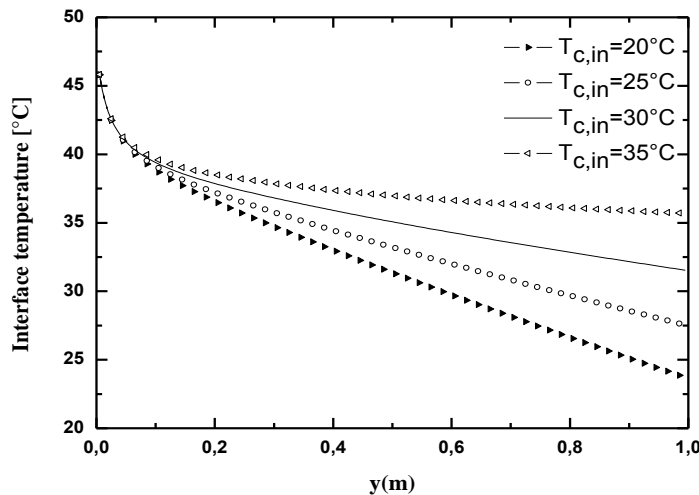


Figure 19. Effect of inlet cooling water temperature on interface temperature at  $T_{in}=45^{\circ}\text{C}$ ,  $W_{in}=0.62$ ,  $Re_{in}=10$  and  $P_{in}=1\text{KPa}$

### CONCLUSION

The process of heat and mass transfer during the absorption of water vapor into an aqueous solution of lithium bromide within a vertical channel was numerically studied. The governing equations of heat and mass transfer are discretized and solved by the finite volume method. The results obtained can be summarized as follows. The temperature across the liquid film increases to the highest at the interface, but the concentration reduces by approaching to the interface. The interface temperature varying rapidly at the inlet region but gradually as  $y$  increase while the wall and bulk temperature varied decreases slowly as  $y$  increases, similarly the interface, wall and bulk concentration change. The results of the effect of operating parameters show that for lower Reynolds number, the absorption mass flux becomes higher at the inlet position. For a higher inlet concentration, the absorption mass flux becomes higher at the inlet then decreases by increasing  $y$ . The inlet pressure increases with an increase in absorption mass flux and the increase in the inlet cooling temperature enhances the absorption mass flux of the water vapor.

## REFERENCES

- [1]. S.Karami and B.Farhanieh, "Numerical modeling of incline plate LiBr absorber," Heat and Mass Transfer, vol.47, 2011, pp. 259-267.
- [2]. Kyung Icksoo, Keith E. Herolda, Yong Tae Kang, "Model for absorption of water vapor into aqueous LiBr flowing over a horizontal smooth tube," International Journal of Refrigeration, vol.30, 2007, pp. 591-600.
- [3]. K. J.Kim, N. S.Berman, D. S.C. Chau, B. D. Wood, "Absorption of water vapor into falling films of aqueous lithium bromide," International Journal of Refrigeration, vol.18, 1995, pp. 486-494.
- [4]. Shoushi Bo, Xuehu Ma, ZhongLan, Jiabin Chen, Hongxia Chen, "Numerical simulation on the falling film absorption process in a counter-flow absorber," Chemical Engineering Journal, vol.156, 2010, pp. 607-612.
- [5]. Md.Raisul Islam, N. E. Wijesundera, J. C.Ho, "Performance study of a falling-film absorber with a film-inverting configuration," International Journal of Refrigeration, vol.26, 2003, pp. 909-917.
- [6]. Marc Medrano, Mahmoud Bourouis, Alberto Coronas, "Absorption of water vapor in the falling film of water-lithium bromide inside a vertical tube at air-cooling thermal conditions," International Journal of Thermal Sciences, vol.41, 2002, pp. 891-898.
- [7]. Liu Yang, Kai Du, XiaofengNiu, Yuan Zhang, Yanjun Li, "Numerical investigation of ammonia falling film absorption outside vertical tube with nanofluids," International Journal of Heat and Mass Transfer, vol.79, 2014, pp. 241-250.
- [8]. WD.Nusselt, oberflächenkondensation des wasserdampfes, ZeitschrVer Deutsch, vol.60, 1916, pp. 541-546.
- [9]. LA. McNeely, "Thermodynamic properties of aqueous solutions of lithium bromide," ASHRAE, Trans.85, 1979, pp. 413-434.
- [10]. S.V. Patankar, "Numerical Heat Transfer and Fluid Flow," Hemisphere Publishing Corporation, 1980.
- [11]. N. Kawae, T. Shigechi, K. Kanemaru, T. Yamada, "Water Vapor Evaporation into Laminar Film Flow of a Lithium Bromide-water Solution (Influence of Variable Properties and Inlet Film Thickness on the Absorption Mass Transfer Rate)," Heat Transfer-Jpn. Res, vol.18, 1989, pp. 58-70.
- [12]. J. I.Yoon, T. T.Phan, Ch. G.Moon, P.Bansal, "Numerical study on heat and mass transfer characteristic of plate absorber," Applied Thermal Engineering, vol.25, 2005, pp. 2219-2235.